

Exploring Ferrocenyl Imine-Phosphane Complexes in Gold(I) Redox Switchable Catalysis and the Role of the “Magic Blue” Oxidant

Juan Carlos Pérez-Sánchez,^a Raquel P. Herrera,^{a,*} and M. Concepción Gimeno^{a,*}

^a Instituto de Síntesis Química y Catálisis Homogénea (ISQCH), Consejo Superior de Investigaciones Científicas (CSIC) – University of Zaragoza, Pedro Cerbuna 12, 50009, Zaragoza, Spain
E-mail: raquelph@unizar.es; gimeno@unizar.es

Manuscript received: May 21, 2024; Revised manuscript received: July 1, 2024;
Version of record online: ■■, ■■



Supporting information for this article is available on the WWW under <https://doi.org/10.1002/adsc.202400593>

© 2024 The Author(s). Advanced Synthesis & Catalysis published by Wiley-VCH GmbH. This is an open access article under the terms of the Creative Commons Attribution Non-Commercial License, which permits use, distribution and reproduction in any medium, provided the original work is properly cited and is not used for commercial purposes.

Abstract: Another class of gold(I) redox-switchable catalysts, incorporating ferrocenyl phosphane-imines, enriches the existing library of gold(I) complexes. Our catalyst proves efficacy in gold(I)-catalyzed cyclizations of furans and benzamides, exhibiting reversible “on-off” switching. Furthermore, we explored the unconventional role of “Magic Blue”, commonly used as an oxidizing agent in various organic transformations, as a potential activator of the Au–Cl bond, initiating conventional gold(I) catalysis.

Keywords: Redox Switchable Catalysis; Ferrocene; Gold(I) Catalysis; Imine-Phosphane; Magic Blue

Introduction

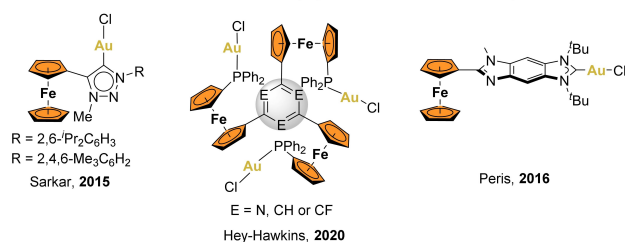
Gold homogeneous catalysis has become an indispensable tool in modern organic synthesis, garnering considerable attention for its unique reactivity and exceptional selectivity in multiple transformations.^[1] The use of a diverse range of ligands to fine-tune the properties of these gold(I) complexes has expanded their synthetic versatility, facilitating the customization of their catalytic performance.^[2] Moreover, homogeneous catalysis seems to stand incomplete without the incorporation of ferrocene. Its unique properties such as electron density, aromaticity, and reversible redox characteristics, make ferrocene a privileged scaffold.^[3]

Despite the significant advancement of gold catalysis,^[4] the synergistic interplay between gold and ferrocene remains relatively underexplored.^[5] The incorporation of the ferrocenyl core within gold catalysts offers several potential advantages, including: a) the robustness and stability of the ligands, b) facile functionalization of the metallocene core, c) high conformational flexibility, d) facile access to chiral

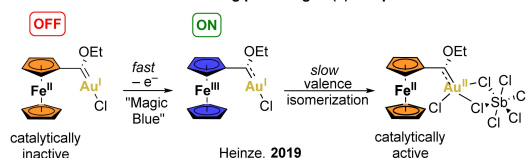
ferrocenyl ligands, and e) the reversible redox properties of ferrocene, enabling redox-switchable catalysis (RSC).^[6] The concept of RSC, pioneered by Wrighton and colleagues in 1995,^[7] relies on adjusting (“switching on and off”) the catalytic activity of a transition metal complex, by manipulating the electron-donating or withdrawing characteristics of a coordinated ligand. Given ferrocene versatility in exhibiting a reversible oxidation process, it frequently serves as the redox-active species in catalytic systems.^[6]

In this context, the groups of Sarkar,^[8] Heinze,^[9] Peris^[10] and Hey-Hawkins^[11] have described a small number of gold(I) complexes bearing pendant ferrocenyl groups, demonstrating their potential as redox switchable catalysts (Scheme 1a). Two possible activation mechanisms behind this concept has been reported: a) The oxidation of the ferrocene moiety, resulting in the generation of a more electron-withdrawing ligand, thereby enhancing the electrophilicity and catalytic activity of the Au(I) center^[7] and b) the formation of a coordinatively unsaturated Fe(II)/Au(II) electromer, which act as a catalytically active putative

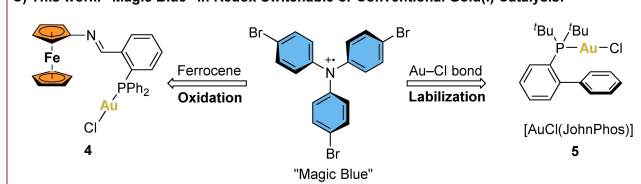
A) Some representative examples of ferrocenyl gold(I) redox switchable catalysts:



B) Proposed activation mechanism involving putative gold(II) complexes:



C) This work: "Magic Blue" in Redox Switchable or Conventional Gold(I) Catalysis:



Scheme 1. a) Representative examples of ferrocenyl gold(I) redox switchable catalysts, b) an example of an activation mode and c) this work.

Au(II) complex (Scheme 1b).^[9a] Moreover, the described complexes are based on ferrocenyl triazole mesoionic carbenes,^[7] Fischer or *N*-heterocyclic carbenes,^[9,10] and tris(ferrocenyl)arene trisphosphane cores.^[11] However, to the best of our knowledge the utilization of ferrocenyl imines remains unexplored (Scheme 1c). Ferrocenyl imines are considered "non-innocent" ligands, capable of inducing strong charge delocalization upon connection by π -linkers. This delocalization facilitates one-electron redox processes, wherein the single electron is delocalized throughout the entire aromatic system.^[12]

In this regard, triarylaminium cations, derived from the oxidation of triaryl amines, have found extensive use as one-electron chemical oxidants due to their strong preference for simple outer-sphere single electron-transfer (SET) reactions.^[13] Thus, the hexachloroantimonate salt of the tris(4-bromophenyl)aminium radical cation, known as "Magic Blue" (Scheme 1c),^[14] has been widely adopted both as a stoichiometric and catalytic oxidant because of its stability, ease of preparation,^[15] commercial availability, and reasonable oxidizing power ($E_{\text{red}} = 0.70 \text{ V vs. Fc}^+/\text{Fc}$).^[16] Nonetheless, its potential applications beyond its role as an oxidant have yet to be explored.

Herein, we present the synthesis of a chloride gold(I) ferrocenyl imine-phosphane complex as another class of gold(I) redox-switchable catalyst. The

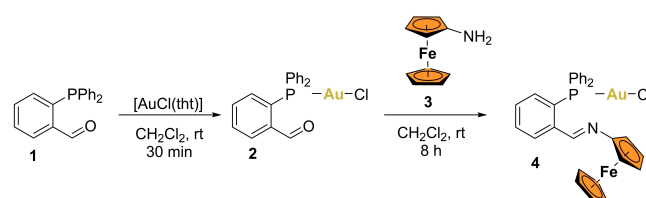
efficacy of this catalyst has been evaluated, employing "Magic Blue" as an oxidant. Intriguingly, we also explored an additional role for "Magic Blue" highlighting its potential ability to activate the Au–Cl bond. To elucidate the comparative activation mechanisms of gold complexes *via* oxidation or halide abstraction, we contrasted the catalytic performance of this ferrocene complex, activated by oxidation, against that of the ubiquitous [AuCl(JohnPhos)] in conventional gold(I) homogeneous catalysis, using "Magic Blue" as the initiator.

Results and Discussion

Firstly, the synthesis of the gold(I) complex was carried out by reacting commercial phosphanebenzaldehyde **1** with [AuCl(tht)] (tht = tetrahydrothiophene), resulting in complex **2** (Scheme 2).

The ^1H NMR spectrum shows the resonance of the aldehyde proton at around 10.30 ppm as a doublet, due to a small coupling ($^4J_{\text{HP}} = 5 \text{ Hz}$) with the phosphorus atom (Figure S1). In the $^{31}\text{P}\{^1\text{H}\}$ spectrum, complex **2** displays a singlet resonating at $\delta_{\text{P}} = 32.0 \text{ ppm}$ (Figure S2). A notable deshielding effect is observed upon coordination of the gold center, compared to the free phosphane ($\delta_{\text{P}} = -11.7 \text{ ppm}$). Subsequently, the synthesis of the ferrocenyl imine involves the reaction of complex **2** with aminoferrocene **3** (Scheme 2). This reaction gives complex **4** in high yield, as a magenta solid, stable both in solid and solution states. In the ^1H NMR spectrum, resonances from the ferrocene group appear in the range of 4.50–3.50 ppm. The imine proton shifts to lower frequencies, appearing around 9.30 ppm (Figure S3), which represents a displacement of approximately $\Delta\delta_{\text{H}} = 1.20 \text{ ppm}$ compared to the aldehyde complex. Additionally, the incorporation of the electron-rich ferrocene moiety leads to significant shielding in the $^{31}\text{P}\{^1\text{H}\}$ spectrum as complex **4** displays a singlet at $\delta_{\text{P}} = 28.6 \text{ ppm}$, corresponding to a displacement of $\Delta\delta_{\text{P}} = -3.4 \text{ ppm}$ (Figure S4).

Complex **4** was further characterized by cyclic voltammetry (see ESI for more information). It displays both single reversible oxidation ($\text{Fe}^{\text{II}} \rightarrow \text{Fe}^{\text{III}}$) and reduction waves ($\text{Fe}^{\text{III}} \rightarrow \text{Fe}^{\text{II}}$), centered on the ferrocene unit (Figure 1a). It exhibits a half-wave potential value of 92.5 mV (see Table S1), slightly



Scheme 2. Synthesis of the ferrocenyl imine-phosphane gold(I) complex **4**.

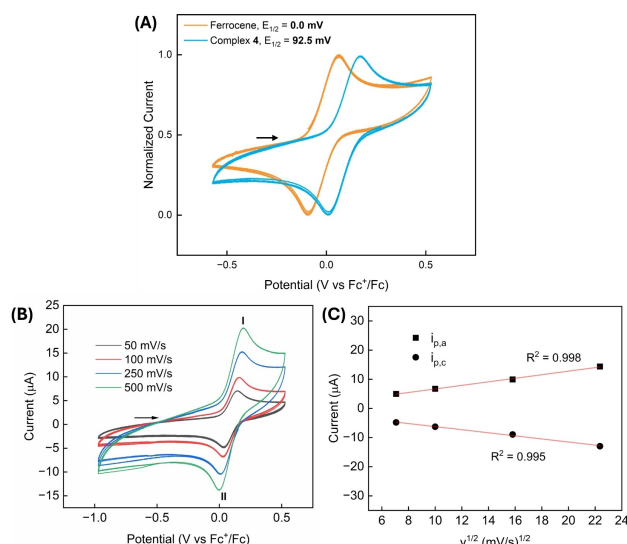


Figure 1. A) Superimposition of cyclic voltammograms of 0.5 mM solutions of complex **4** (blue) and ferrocene (orange) in $\text{CH}_2\text{Cl}_2/0.1 \text{ M } [\text{Bu}_4\text{N}][\text{PF}_6]$ at 250 mV/s, referenced against Fc^+/Fc couple. B) Superimposition of cyclic voltammograms recorded at different scan rates (50–500 mV/s). C) Relationship between peak current (i_p) and the square root of scan rate ($v^{1/2}$) (Randles–Ševčík equation) for the anodic (black squares, peak I) and cathodic (black circles, peak II) peaks. Linear fits are shown in red.

surpassing those of the reference ferrocene ($E_{1/2} = 0.0 \text{ mV}$) and around 400 mV anodically shifted from aminoferrocene ($E_{1/2} = -310.5 \text{ mV}$ against Fc^+/Fc).^[16] This deviation suggests an enhanced electron donation from the ferrocene fragment to the gold complex upon imine formation, consequently leading to a reduction in electron density on the ferrocene unit. Moreover, all voltammograms recorded at different scan rates ranging from 50 to 500 mV/s (Figure 1b), were fitted to the Randles–Ševčík equation (Figure 1c), supporting the chemical reversibility of the system. Similarly, the cathodic process and anodic processes demonstrated similar current peak intensities, as evidenced by the $i_{p,a}/i_{p,c}$ ratio approximating 1 (with an average value of 1.08), confirming this chemical reversibility of the $\text{Fe}^{\text{II}} \leftrightarrow \text{Fe}^{\text{III}}$ transitions (see Table S2).

Additionally, it is noteworthy that the separation between the anodic peak potentials ($E_{p,a}$) and cathodic peak potentials ($E_{p,c}$) exceeded ($\Delta E_p = 174 \text{ mV}$) the theoretical value predicted by the Nernst equation, typically $59/n \text{ mV}$, where n represents the number of electrons involved in the redox process (see Table S1). This deviation could be attributed to increased solution resistance in the analyzed solution as peak-to-peak separation for Fc^+/Fc is $\Delta E_p = 162 \text{ mV}$ in the same cyclic voltammogram.

Furthermore, single crystal X-ray diffraction revealed that complex **4** crystallizes as a dichloromethane solvate (Figure 2).

The gold(I) center adopts a linear coordination environment, with a P1-Au1-Cl1 angle of $178.43(5)^\circ$. The crystal structure reveals that the imine exists as the *E* isomer, consistent with its conformation in solution as indicated by the ^1H – ^1H NOESY spectrum of **4** (Figure S9). This spectrum shows two cross-peaks from the imine proton, one with the *ortho* proton of the phenyl ring and the other one with the protons from the Cp ring. Notably, a short contact is observed between the gold(I) center and the nitrogen atom with a distance of $3.035(4) \text{ \AA}$ (Table S5).

Following the synthesis of the gold complexes, their catalytic activity was tested in two benchmark reactions in gold(I) catalysis: the intramolecular cyclization of furans and propargyl amides to give phenols^[17] (Table 1) and oxazolines^[18] (Table 2), respectively. Initially, we investigated the cyclization of furan **6a** to phenol **8a** using complex **4**. Full conversion was achieved within 3 hours; however, the yield was moderate (Table 1, entry 1). This moderate yield may be attributed to an undesired side reaction leading to the intermolecular polymerization of substrate **6a**, as previously described by Shi and co-workers on these furan-ynes.^[19] As the authors reported, when employing dilution factors ($[\mathbf{6a}] = 0.08 \text{ M}$ or $[\mathbf{6a}] = 0.04 \text{ M}$), a slight increase in yield was observed (Table 1, entries 2 and 3). Subsequently, we explored the cyclization of substrate **7a**. After obtaining promising preliminary results, a solvent screening was conducted, revealing dichloromethane as the optimal solvent (Table S3). Complex **4** gave **9a**

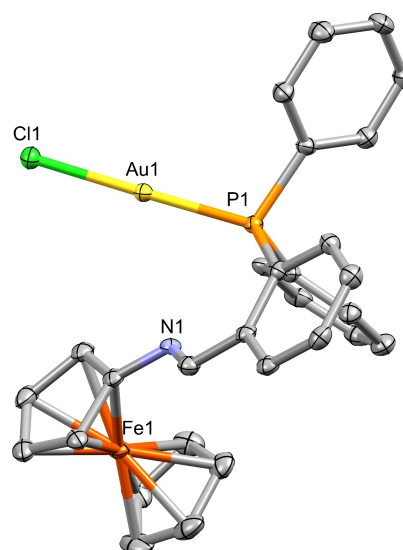
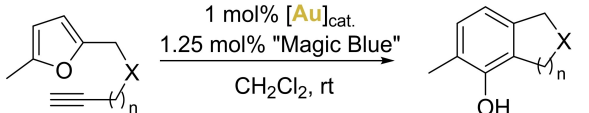


Figure 2. Crystal structure of complex **4** · CH_2Cl_2 . Ellipsoids are shown at 50% probability level. Hydrogen atoms and a dichloromethane molecule are omitted for clarity.

Table 1. Catalytic results of the 5-*exo-dig* cyclization of furans (6–7) to phenols (8–9).

				
6a: X = O, n = 1				8a: X = O, n = 1
7a: X = NTs, n = 1				9a: X = NTs, n = 1
7b: X = NTs, n = 2				9b: X = NTs, n = 2
Entry ^[a]	Substrate	[Au] _{cat.}	Time (h)	Yield ^[b] (%)
1	6a	4	3	46 ^[c]
2	6a ^[d]	4	24	52
3	6a ^[e]	4	24	60
4	6a	2	3	10
5	6a	5	3	12
6	7a	4	6	78 ^[c]
7	7a	4	14	96
8	7b	4	14	15
9	7a	4	14	93 ^[e]
10	7a	2 ^[f]	24	n.r.
11	7a	4 ^[f]	24	n.r.
12	7a	3 ^[f]	24	n.r.
13	7a	3	24	n.r.
14	7a	None	24	n.r.
15	7a	2	6	15
16	7a	5	6	27
17	7a	5 ^[f]	6	n.r.

^[a] Reaction conditions: 0.1 mmol of substrate, 0.001 mmol (1 mol%) catalyst, 0.00125 mmol (1.25 mol%) oxidant ("Magic Blue"), 0.5 mL of CH₂Cl₂, 20–25 °C (rt).

^[b] Determined by ¹H NMR using 1,3,5-trimethoxybenzene as internal standard.

^[c] Isolated yield after column chromatography.

^[d] 0.2 mmol of substrate in 2.5 mL of CH₂Cl₂.

^[e] 0.2 mmol of substrate in 5 mL of CH₂Cl₂.

^[f] No oxidant. n.r. = no reaction.

^[g] Reaction at one gram scale (3.5 mmol).

in 78% yield within 6 hours (Table 1, entry 6), which increased to nearly quantitative 96% yield after 14 hours (Table 1, entry 7). Extending the carbon chain length on furan **7** from prop-2-yne **7a** to but-3-yne **7b** significantly reduced catalytic activity, resulting in a 15% yield of compound **9b** over 14 hours (Table 1, entry 8). Interestingly, increasing the amount of substrate **7a** to gram scale (35 times more) did not significantly alter the yield (Table 1, entry 9), demonstrating the scalability of the methodology. Pure product **9a** was easily obtained by filtering the precipitate from the crude mixture followed by washing the solid with cold dichloromethane.

We also conducted some background reactions using complex **2** and aminoferrocene **3**, both in the presence and absence of "Magic Blue" (Table 1, entries 10–17). As anticipated, complexes **2** and **4** were inactive without "Magic Blue" (Table 1, entries 10 and

11). Furthermore, both **3** and aminoferrocenium cation, generated *in situ* from **3** and "Magic Blue", did not yield the cyclization product (Table 1, entries 12 and 13), also "Magic Blue" itself exhibited no reactivity (Table 1, entry 14).

Unexpectedly, when complex **2** was tested in the presence of "Magic Blue" (Table 1, entry 15), a 15% yield was achieved within 6 hours. This intriguing result prompted us to further investigate the role of "Magic Blue" in this redox catalysis. It appears that "Magic Blue" may function both as an oxidant or as a chloride scavenger, initiating conventional gold(I) catalysis, depending on the gold(I) complex tested. To further explore this hypothesis, we evaluated the well-known gold(I) complex [AuCl(JohnPhos)] **5** (JohnPhos = [1,1'-biphenyl]-2-yl-di-tertbutylphosphane), in these reactions. Indeed, it resulted to be catalytically active, yielding 27% of product **9a** in 6 hours (Table 1, entry 16). In contrast, in the absence of oxidant, **5** did not yield phenol **9a** (Table 1, entry 17).

As discussed, the role of "Magic Blue" in the presence of this gold(I) chloride complex may engage the Au–Cl bond, with a subsequent labilization, probably due to a weak intermolecular Au–Cl→N⁺ interaction, the formation of which benefits from a possible pnictogen bond (with a deeper π-hole) or a higher Lewis acidic properties of the radical cation compared to a conventional ammonium salt.^[20] To gain insight into the activation process, we investigated the interaction between **5** and "Magic Blue" using ³¹P{¹H} NMR spectroscopy to monitor chemical shift changes. Upon mixing equimolar amounts of **5** and "Magic Blue" in CD₂Cl₂, a chemical shift of Δδ_p = +0.23 ppm was observed compared to free **5** (δ_p = 60.07 ppm), accompanied by broadening of the phosphorus signal, with a Δω_{1/2} = +25.5 Hz, compared to the value for complex **5**, ω_{1/2} = 3.7 Hz (see Figure S28). As previously reported by Fiksdahl and Erdelyi,^[21] the presence of a charge transfer *via* halogen bonding, possibly through pnictogen bonding in this case, leads to a depletion of electron density around the phosphorus atom. This results in a positive chemical shift difference between the free complex and the mixture in the presence of "Magic Blue".

With these results in hand, we further investigated the kinetic profiles of complexes **2**, **4**, and **5** in the presence of "Magic Blue". Additionally, we employed NaBAR₄^F (BAR₄^F = tetrakis[3,5-bis(trifluoromethyl)phenyl]borate),^[22] a silver-free anion abstractor, as a non-oxidizing chloride scavenger, in combination with complex **4** (Figure 3).

Both gold(I) complexes **2** (TOF = 5.7 × 10^{−4} s^{−1}) and **5** (TOF = 1.1 × 10^{−3} s^{−1}) exhibited the slowest reaction rates.^[23] Notably, the catalytic activity of **5** was almost two times higher than that for **2**. In contrast, complex **4** demonstrated the highest conversion rates for the cyclization of **7a** (Figure 3). Specifically, the catalytic

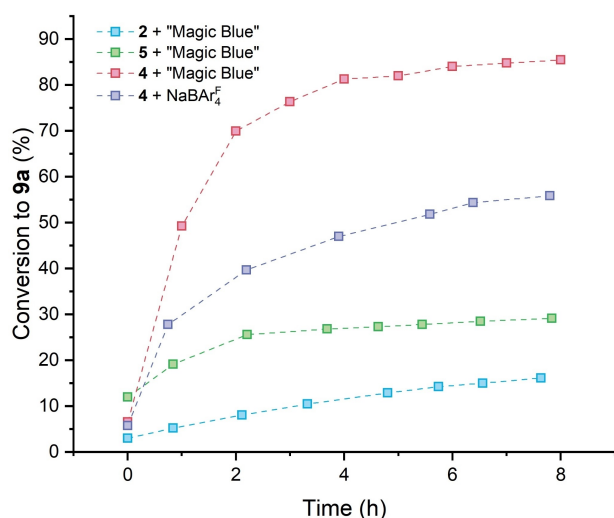


Figure 3. Conversion for the cyclization of **7a** to **9a** as a function of reaction time, employing complexes **2**, **4** and **5**.

activity of **4** in presence of "Magic Blue" ($\text{TOF} = 3.0 \times 10^{-3} \text{ s}^{-1}$) was 5.3 times higher than that of **2**. The incorporation of the redox-active ferrocene moiety in **4**, markedly increases the reaction rate, indicating that this complex can be activated *via* a straightforward oxidation step. This activation significantly enhances the activity in the gold(I)-catalyzed cyclization process, in contrast to complex **2**, where "Magic Blue" initiates gold(I) catalysis by possibly inducing Au–Cl bond lability. Furthermore, in the presence of NaBAR_4 , complex **4** ($\text{TOF} = 2.0 \times 10^{-3} \text{ s}^{-1}$) exhibited a lower catalytic activity compared to its activation through oxidation. However, it demonstrated superior activity compared to the activation of complexes **2** and **5** using "Magic Blue", suggesting that this aminium radical cation is a less efficient chloride scavenger than the BAR_4^{F} anion. Notably, the redox activation of complex **4** outperformed all other activation methods, resulting in 1.5 times increase in activity compared to conventional halide abstraction (Figure 3). This improvement is further evidenced by higher conversion values observed, within the first hour, for complex **4** when activated by "Magic Blue", compared to its activation by $\text{NaBAR}_4^{\text{F}}$.

Then, we evaluated the redox-switchable catalysis capability of complex **4**, given its electrochemically reversible oxidation process (Figure S30). Decamethylferrocene (FeCp_2^*) was selected as the reducing agent due to its common use in RSC studies and its compatibility with the catalytic system (Figure 4).

Upon examination of the NMR spectra, the catalytic process progressed in two differentiated phases over a nine-hour period. Initially, the introduction of "Magic Blue" served as a catalyst "switch on", triggering a gradual increase in substrate conversion. After 1 hour, approximately 50% of the substrate was

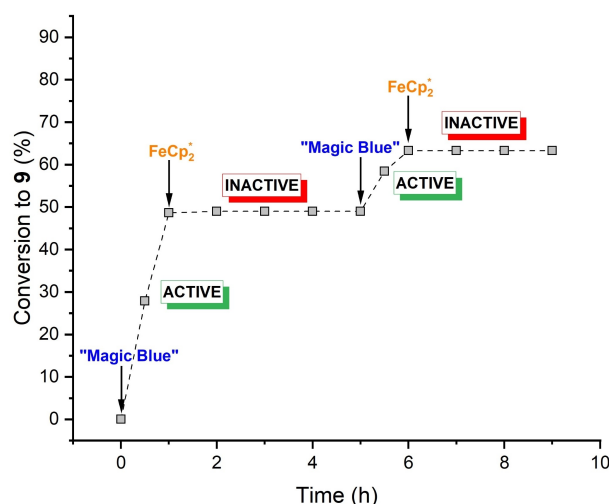


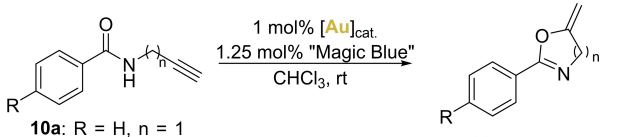
Figure 4. Conversion *versus* time plot of the cyclization of **7a** to **9a** during redox switchable catalysis using "Magic Blue" (1.25 mol% respect to **4**) and FeCp_2^* (1.25 mol% respect to **4**). Arrows indicate the time points at which said reagents were added to the reaction mixture.

converted to the desired product (Figure 4). The later addition of FeCp_2^* , effectively "switches off" the catalytic activity. Subsequent monitoring over the next 4 hours revealed no further conversion, confirming catalyst deactivation. To reinstate the catalytic cycle, a second addition of "Magic Blue" was introduced to the reaction mixture. This reignited the catalytic activity, leading to increased substrate conversion to approximately 65% within the next hour. A second batch of the reducing agent halted the catalytic activity of complex **4** once again over the last 3 hours. This alternating "on-off-on-off" switching pattern (Figure 4) highlights the reversible nature of this catalytic system, offering an additional class of gold(I) redox-switchable catalysts to the existing library of such complexes.

To expand the catalytic activity of the ferrocenyl-imine phosphane **4**, we evaluated its performance in another common gold(I)-catalyzed reaction: the cyclization of propargyl benzamides (**10a–d**) to oxazolines (**11a–c**). The results revealed that the catalytic performance of the tested complexes varied significantly (Table 2).

Compared to complexes **2** and **5**, complex **4** demonstrated superior catalytic activity. Within 14 hours, half of the substrate had been converted (Table 2, entry 1), and by 24 hours, oxazolines **11a–c** were obtained with comparable isolated yields (Table 2, entries 2–4). Interestingly, the presence of either electron-withdrawing or electron-donating substituents on benzamides **10b** and **10c** respectively, did not significantly affect the yield (Table 2, entries 3 and 4). In this case, as observed previously, homologating the carbon chain length from a propargyl group to a

Table 2. Catalytic results of the 5-*exo-dig* cyclization of propargyl amides (**10 a–d**) to oxazolines (**11 a–c**).



10a: R = H, n = 1
10b: R = F, n = 1
10c: R = Me, n = 1
10d: R = H, n = 2

11a: R = H, n = 1
11b: R = F, n = 1
11c: R = Me, n = 1

Entry ^[a]	Substrate	[Au] _{cat.}	Time (h)	Yield ^[b] (%)
1	10 a	4	14	51
2	10 a	4	24	74 ^[c]
3	10 b	4	24	71 ^[c]
4	10 c	4	24	70 ^[c]
5	10 d	4	24	n.r. ^[d]
6	10 a	2	14	6
7	10 b	2	14	8
8	10 a	5	14	10
9	10 b	5	14	9

^[a] Reaction conditions: 0.1 mmol of substrate, 0.001 mmol (1 mol%) catalyst, 0.00125 mmol (1.25 mol%) oxidant ("Magic Blue"), 0.5 mL of CHCl₃, 20–25 °C (rt).

^[b] Determined by ¹H NMR using 1,3,5-trimethoxybenzene as internal standard.

^[c] Isolated yield after column chromatography.

^[d] n.r. = no reaction.

homopropargyl group resulted in a loss of catalytic activity for complex **4** under our conditions. This significant decrease in reactivity was unexpected and suggests that the extended carbon chain may interfere with the cyclization process or the interaction with the catalyst.

In contrast to complex **4**, complexes **2** and **5** yielded oxazolines with less than 10% yield within 14 hours (Table 2, entries 5–9). These findings highlight the enhanced catalytic performance and broader applicability of redox activation in complex **4**, surpassing the Au–Cl bond labilization induced by "Magic Blue" in complexes **2** and **5**.

Conclusion

In summary, we have introduced an example to the array of gold(I) redox-switchable catalysts, featuring a ferrocenyl phosphane-imine core. This complex displays efficiency in catalyzing gold(I)-mediated cyclizations of furans and benzamides, showcasing its reversible "on-off" switching capability. Furthermore, our exploration exposed a potential dual role for "Magic Blue", traditionally recognized just as an oxidizing agent. When a redox-active fragment (*e.g.*, ferrocene) is integrated into the complex, it acts as a one-electron oxidant, thereby initiating an oxidation-activated catalysis, which can be switched on and off

by the addition of an oxidizing or reducing agent, respectively. Moreover, in cases where the gold(I) complex fails to initiate an oxidation process, "Magic Blue" exhibits potential as a Au–Cl bond labilizing agent, though with modest activity, in conventional gold(I) catalysis.

Experimental Section

Synthesis of Complex 2

This compound was synthesized following a modified literature procedure.^[24] In a 50 mL round bottom flask, **2** (diphenylphosphane)benzaldehyde **1** (58 mg, 0.2 mmol) was dissolved in CH₂Cl₂ (20 mL). Then, [Au(Cl)(tht)] (64 mg, 0.2 mmol) was added and the resulting yellow solution turned colorless within a few minutes. Then, the solution was stirred for 30 min. After this time, the solvent was evaporated under reduced pressure to *ca.* 1 mL and *n*-hexane (10 mL) was added, precipitating a white solid. The resulting solid was purified through washings with *n*-hexane (2×5 mL) and dried under vacuum.

Synthesis of Complex 4

To a flame dried Schlenk flask equipped with a stirring bar was added 20 mg of molecular sieve (4 Å) and dry and degassed CH₂Cl₂ (20 mL). Under an argon flow, **2** (78 mg, 0.15 mmol) was added. Then aminoferrocene **3** (35 mg, 0.165 mmol) and 3 drops of acetic acid, were added and the resulting orange solution was stirred for 8 hours. After this time, the solution turned dark magenta, and it was filtered by a canula filter. Then, the solvent was reduced under reduced pressure to *ca.* 1 mL and propan-2-ol (10 mL) was added, precipitating a magenta solid. The resulting solid was purified through washings with propan-2-ol (1×5 mL), *n*-hexane (2×5 mL) and dried under vacuum. Crystals suitable for X-ray studies were obtained by vapor diffusion of *n*-hexane over a solution of **4** in dichloromethane.^[25]

General Procedure for the Study of Gold(I)-Catalyzed Cyclizations

In a 5 mL scintillation vial, the substrate (0.2 mmol) was dissolved in the corresponding volume of CH₂Cl₂. Next, the solid catalyst (0.0020 mmol, 1 mol%) was added to the solution, resulting in the immediate dissolution of the catalyst, and forming a violet solution. Then, the solid oxidant, "Magic Blue" (0.0025 mmol, 1.25 mol%), was added, and the solution immediately turned yellow. The mixture was stirred at room temperature for the time needed for total consumption of the starting reagent or until no further progress was observed (24 h), monitoring the evolution by thin-layer chromatography (*n*-hexane/ethyl acetate, 7:3). After the specified time, the isolated yields were determined by purifying the crude products using flash column chromatography (SiO₂, *n*-hexane/ethyl acetate, 8:2). The purified products were analyzed by ¹H NMR, and the spectroscopic data agreed with previously reported literature.^[18a,26,27]

General Procedure for the Study of Gold(I)-Redox Switchable Catalysis

In a 5 mL scintillation vial, a mixture of substrate **7a** (0.1 mmol) and 1,3,5-trimethoxybenzene (0.011 mmol) in 0.5 mL of CD₂Cl₂ was prepared. Subsequently, **4** (0.001 mmol, corresponding to 1 mol% of Au) was added. The progress of the reaction was monitored using ¹H NMR spectroscopy on a Bruker ARX300 instrument with a constant temperature of 25 °C. Over a period of 9 hours, one ¹H NMR experiment, each consisting of 32 scans (161 seconds), was conducted at hourly intervals to track the reaction progression. For each measurement, an aliquot of ca. 10 µL of the reaction mixture was transferred to an NMR tube, and it was quenched by the addition of 0.45 mL of MeOD. To “switch on” the reaction, solid “Magic Blue” (0.0125 mmol, corresponding to 1.25 mol% relative to the catalyst) was added to the mixture. To “switch off” the reaction, solid FeCp₂* (0.0125 mmol, corresponding to 1.25 mol% relative to the catalyst) was added to the reaction mixture. For the evaluation of conversion and yield see Supporting Information (Figure S31).

Acknowledgements

The authors thank projects PID2022-136861NB-I00 and PID2020-117455GB-I00 funded by MICIU/AEI/10.13039/501100011033, and Gobierno de Aragón (Research Group E07_23R). We acknowledge support of the publication fee by the CSIC Open Access Publication Support Initiative through its Unit of Information Resources for Research (URICI). J. C. Pérez-Sánchez also thanks the Spanish Ministerio de Ciencia, Innovación y Universidades MICIU for a predoctoral grant (FPU21/01888).

References

- [1] a) *Modern Gold Catalyzed Synthesis*; A. S. K. Hashmi, F. D. Toste, (Eds.); Wiley-VCH, Weinheim, **2012**; b) R. P. Herrera, M. C. Gimeno, *Chem. Rev.* **2021**, *121*, 8311–8363.
- [2] A. Collado, D. J. Nelson, S. P. Nolan, *Chem. Rev.* **2021**, *121*, 8559–8612.
- [3] a) A. Fihri, P. Meunier, J.-C. Hierso, *Coord. Chem. Rev.* **2007**, *251*, 2017–2055; b) K. Heinze, H. Lang, *Organometallics* **2013**, *32*, 5623–5625; c) D. Astruc, *Eur. J. Inorg. Chem.* **2017**, 2017, 6–29.
- [4] For recent reviews concerning silver-free Au(I) catalysts activation protocols, see: a) A. Franchino, M. Montesinos-Magraner, A. M. Echavarren, *Bull. Chem. Soc. Jpn.* **2021**, *94*, 1099–1117; b) J. C. Pérez-Sánchez, R. P. Herrera, M. C. Gimeno, *Chem. A Eur. J.* **2024**, e202401825, DOI 10.1002/chem.202401825.
- [5] J. C. Pérez-Sánchez, R. P. Herrera, M. C. Gimeno, *Chem. - Eur. J.* **2024**, *30*, e202303585.
- [6] J. C. Pérez-Sánchez, R. P. Herrera, M. C. Gimeno, *Eur. J. Inorg. Chem.* **2022**, 2022, e202101067.
- [7] I. M. Lorkovic, R. R. Jr Duff, M. S. Wrighton, *J. Am. Chem. Soc.* **1995**, *117*, 3617–3618.
- [8] a) L. Hettmanczyk, S. Manck, C. Hoyer, S. Hohloch, B. Sarkar, *Chem. Commun.* **2015**, *51*, 10949–10952; b) L. Hettmanczyk, L. Suntrup, S. Klenk, C. Hoyer, B. Sarkar, *Chem. A Eur. J.* **2017**, *23*, 576–585; c) S. Vanicek, M. Podewitz, J. Stubbe, D. Schulze, H. Kopacka, K. Wurst, T. Müller, P. Lippmann, S. Haslinger, H. Schottenberger, K. R. Liedl, I. Ott, B. Sarkar, B. Bildstein, *Chem. A Eur. J.* **2018**, *24*, 3742–3753.
- [9] a) P. Veit, C. Volkert, C. Förster, V. Ksenofontov, S. Schlicher, M. Bauer, K. Heinze, *Chem. Commun.* **2019**, *55*, 4615–4618; b) M. P. Schrick, G. K. Ramollo, C.-M. S. Hirschbiegel, M. Fernandes, A. Lemmerer, C. Förster, D. I. Bezuidenhout, K. Heinze, *Organometallics* **2024**, *43*, 69–84.
- [10] S. Ibáñez, M. Poyatos, L. N. Dawe, D. Gusev, E. Peris, *Organometallics* **2016**, *35*, 2747–2758.
- [11] a) A. Straube, P. Coburger, L. Dütsch, E. Hey-Hawkins, *Chem. Sci.* **2020**, *11*, 10657–10668; b) A. Straube, P. Coburger, M. Michak, M. R. Ringenberg, E. Hey-Hawkins, *Dalton Trans.* **2020**, *49*, 16667–16682.
- [12] C. Carter, Y. Kratish, T. Jurca, Y. Gao, T. J. Marks, *J. Am. Chem. Soc.* **2020**, *142*, 18715–18729.
- [13] N. G. Connelly, W. E. Geiger, *Chem. Rev.* **1996**, *96*, 877–910.
- [14] a) F. A. Bell, A. Ledwith, D. C. Sherrington, *J. Chem. Soc. C* **1969**, *77*, 2719–2720; b) M. Quiroz-Guzman, S. N. Brown, *Acta Crystallogr. Sect. C* **2010**, *66*, m171–m173.
- [15] a) M. R. Talipov, M. M. Hossain, A. Boddeda, K. Thakur, R. Rathore, *Org. Biomol. Chem.* **2016**, *14*, 2961–2968; b) K. Keshari, M. Bera, L. Velasco, S. Munshi, G. Gupta, D. Moonshiram, S. Paria, *Chem. Sci.* **2021**, *12*, 4418–4424; c) F. Wu, J. Xu, H. Gao, C. Li, S. Xu, H. Uno, Y. Xu, Y. Zhao, Z. Shen, *Chem. Commun.* **2021**, *57*, 383–386.
- [16] K. Heinze, M. Schlenker, *Eur. J. Inorg. Chem.* **2004**, *2004*, 2974–2988.
- [17] a) A. S. K. Hashmi, T. M. Frost, J. W. Bats, *J. Am. Chem. Soc.* **2000**, *122*, 11553–11554; b) A. S. K. Hashmi, T. M. Frost, J. W. Bats, *Org. Lett.* **2001**, *3*, 3769–3771; c) A. S. K. Hashmi, T. M. Frost, J. W. Bats, *Catal. Today* **2002**, *72*, 19–27; d) A. S. K. Hashmi, M. C. Blanco, E. Kurpejovic, W. Frey, J. W. Bats, *Adv. Synth. Catal.* **2006**, *348*, 709–713; e) A. S. K. Hashmi, M. Rudolph, H.-U. Siehl, M. Tanaka, J. W. Bats, W. Frey, *Chem. A Eur. J.* **2008**, *14*, 3703–3708; f) A. S. K. Hashmi, M. Rudolph, J. Huck, W. Frey, J. W. Bats, M. Hamzic, *Angew. Chem. Int. Ed.* **2009**, *48*, 5848–5852.
- [18] a) J. P. Weyrauch, A. S. K. Hashmi, A. Schuster, T. Hengst, S. Schetter, A. Littmann, M. Rudolph, M. Hamzic, J. Visus, F. Rominger, W. Frey, J. W. Bats, *Chem. A Eur. J.* **2010**, *16*, 956–963; b) A. S. K. Hashmi, M. C. B. Jaimes, A. M. Schuster, F. Rominger, *J. Org. Chem.* **2012**, *77*, 6394–6408; c) D. Hueber, M. Hoffmann, P. de Frémont, P. Pale, A. Blanc, *Organometallics* **2015**, *34*, 5065–5072; d) B. Zhou, F. P. Gabbaï, *J. Am. Chem. Soc.* **2021**, *143*, 8625–8630; e) N. V. Tzouras, L. P. Zorba, E. Kaplanai, N. Tsoareas, D. J. Nelson, S. P.

- Nolan, G. C. Vougioukalakis, *ACS Catal.* **2023**, *13*, 8845–8860; f) W.-C. Liu, F. P. Gabbaï, *Chem. Sci.* **2023**, *14*, 277–283.
- [19] Y. Chen, W. Yan, N. G. Akhmedov, X. Shi, *Org. Lett.* **2010**, *12*, 344–347.
- [20] B. Lin, H. Liu, I. Karki, E. C. Vik, M. D. Smith, P. J. Pellechia, K. D. Shimizu, *Angew. Chem. Int. Ed.* **2023**, *62*, e202304960.
- [21] H. F. Jönsson, D. Sethio, J. Wolf, S. M. Huber, A. Fiksdahl, M. Erdelyi, *ACS Catal.* **2022**, *12*, 7210–7220.
- [22] a) H. Nishida, N. Takada, M. Yoshimura, T. Sonoda, H. Kobayashi, *Bull. Chem. Soc. Jpn.* **1984**, *57*, 2600–2604; b) M. R. Frutos, T. R. Belderrain, P. de Frémont, N. M. Scott, S. P. Nolan, M. M. Díaz-Requejo, P. J. Pérez, *Angew. Chem. Int. Ed.* **2005**, *44*, 5284–5288.
- [23] The determined TOFs, calculated as TON/time, are based on the conversion versus time plot (Figure 3) at *ca.* 8 h. Here, TON (mmol product/mmol catalyst) equals the conversion value (%), at the exact time point it was measured, considering the catalyst loading is 1 mol%.
- [24] M. R. J. Elsegood, M. B. Smith, S. H. Dale, *Acta Crystallogr. Sect. E* **2006**, *62*, m1850–m1852.
- [25] CCDC deposition number 2352316 (4), contains the supplementary crystallographic data. These data can be obtained free of charge by The Cambridge Crystallography Data Center via www.ccdc.cam.ac.uk/structures.
- [26] C. Nieto-Oberhuber, S. López, A. M. Echavarren, *J. Am. Chem. Soc.* **2005**, *127*, 6178–6179.
- [27] S. Nejrotti, F. Marra, E. Priola, A. Maranzana, C. Prandi, *J. Org. Chem.* **2021**, *86*, 8295–8307.

RESEARCH ARTICLE

Exploring Ferrocenyl Imine-Phosphane Complexes in Gold(I) Redox Switchable Catalysis and the Role of the “Magic Blue” Oxidant

Adv. Synth. Catal. **2024**, *366*, 1–9

J. C. Pérez-Sánchez, R. P. Herrera*, M. C. Gimeno*

